Technical note: An operational implementation of recursive digital filter for baseflow separation

Mohamad Rammal[12], Pierre Archambeau[2], Sebastien Erpicum[2], Philippe Orban[3], Serge Brouyère[3], Michel Pirotton[2], Benjamin Dewals[2]

Key points:

1. A practical, automatic, and reproducible procedure to calibrate the recursive digital filter can be attained using an original objective function
2. Comparison tests between several watersheds and between different separation techniques demonstrate the validity and robustness of our approach
3. The developed method offers a more operational alternative to the standard graphical one and a less expensive way than more elaborate methods

Abstract. Baseflow estimation is of overwhelming importance in hydrological modelling and water resources management. One of the widely used techniques to derive baseflow from measured stream flow is the Recursive Digital Filter (RDF). Yet its application still raises methodological issues related to the determination of its parameters. In this study, we propose a practical and automatic procedure to calibrate the RDF with respect to the measured stream flow. The method operationality and robustness are first demonstrated on three gauging stations in the Ourthe catchment (Belgium). The calibrated parameters compare well with those obtained by a standard graphical approach. Next, the proposed approach is compared to the technique of Conductance Mass Balance (CMB) for two gauging stations in the Hoyoux catchment (Belgium). A fair agreement between the results of the two techniques is obtained, suggesting that the proposed automatic calibration procedure of RDF takes the baseflow separation process to a higher level of practicality and transparency.

Keywords. Baseflow, optimization, objective function, recursive digital filter, conductance mass balance, recession rate

[1] Corresponding author (mohamad.rammal@uliege.be)

[2] Hydraulics in Environmental and Civil Engineering (HECE), University of Liège (ULiège), Liège, 4000, Belgium
[3] Hydrogeology and Environmental Geology (HGE), University of Liège (ULiège), Liège, 4000, Belgium

1 Introduction

Baseflow represents the groundwater contribution to stream flow (Halford and Mayer, 2000; Hall, 1968; Rutledge, 1997). Unlike stream flow rate, the direct measurement of baseflow is practically impossible (e.g. Tardy et al., 2004). However, baseflow plays a critical role in understanding water budgets (Arnold and Allen, 1999; Stewart et al., 2007), analyzing water cycle vulnerability to natural and anthropological effects (Tesoriero et al., 2013), improving management strategies of water supply systems and underground water protection (e.g. Wenninger et al., 2004), and implementing process-based hydrological models in an objective way (Beven, 1989; Eckhardt et al., 2002; Ferket et al., 2010; Lang et al., 2008; Willems, 2014). This explains the plethora of techniques that have been proposed to estimate baseflow (see Hall (1968) and Tallaksen (1995) for comprehensive reviews).

The most common methods are the graphical ones that rely on stream discharge data alone. They use either the recession-curve-displacement technique (Barnes, 1939; Daniel, 1976; Rorabaugh, 1964) or a low-pass filter (Chapman, 1991; Nathan and McMahon, 1990). The former is based on the exponential solution of the differential equation governing unsteady infiltration flow established by Boussinesq in 1877 (Hall, 1968). Although it is considered more theoretically based than the filter methods, it has been abandoned because of the underlying assumptions concerning the physical properties of the aquifer that limit its validity to ideal cases, i.e. homogeneous, uniform, isotropic and confined aquifers (Halford and Mayer, 2000; Rutledge, 2005). The most widely used low-pass filter is the Recursive Digital Filter (RDF) adapted from signal processing theory (Chapman, 1991; Nathan and McMahon, 1990; Willems, 2009). It was judged as objective (Chapman, 1991) and was highly recommended for its direct link with lumped hydrological representations of watersheds (Willems, 2009). Nonetheless, RDF requires an estimate of the watershed-specific recession constant, which remains difficult to determine.

Early techniques for estimating the recession constant include the matching strip method (Toebes and Strang, 1964) and the correlation method (Langbein, 1938). The first one consists in determining a master recession curve based on the best eye fit of all the individual recession segments superimposed on a semi-logarithmic scale. However, the results may be biased by over- or under-estimations of the actual length of the recession periods, as well as human judgment in the visual inspection of the recession segments (Hall, 1968). Although Nathan and McMahon (1990) succeeded to semi-automatize this procedure, the non-reproducibility issue persisted. In the correlation method (Langbein, 1938), the recession constant is determined by fitting a curve on the discharge values at one time step plotted against the discharge values at a later time step. Nathan and McMahon (1990) tested this approach to find that the uncertainty involved in the curve fitting procedure makes the method unsuitable for the analysis of recession flow. Despite multiple attempts made to improve these methods (Brutsaert and Nieber, 1977; Cheng et al., 2016; Nathan and McMahon, 1990; Rutledge and Daniel, 1994; Singh and Stall, 1971), determining the recession constant still involves a high degree of subjectivity and a lack of reproducibility (Li et al., 2014; Nejadhashemi et al., 2003; Stewart et al., 2007; Tallaksen, 1995; Zhang et al., 2013).

Later studies developed separation techniques that could serve as a reference for RDF calibration and evaluation. One approach relies on additional field measurements, such as the groundwater level (Holko et al., 2002; Peters and Van Lanen, 2005) or the concentration of a conservative geochemical tracer which depends on the flow path (Cey et al., 1998; Gonzales et al., 2009; Matsubayashi et al., 1993; Pilgrim et al., 1979; Pinder and Jones, 1969; Stewart et al.,

2007). The most commonly used tracer is the specific conductance, which is substantially higher for subsurface flow than for surface flow (Li et al., 2014; Zhang et al., 2013). This led to the development of the widely recognized conductance mass balance method (CMB). In another approach, reference baseflow estimates are derived from numerical simulations performed with a physically-based hydrological model, e.g. the HydroGeoSphere (HGS) model (Therrien et al., 2010) used in (Su et al., 2016) to evaluate different RDFs. Despite the promising results obtained by these methods, the additional efforts required to collect more data or to implement complex numerical models make them less attractive in practice, especially for long runs and for past periods for which additional data may be unavailable.

In this paper, we propose an operational procedure to calibrate the RDF parameters without any supplementary experimental or modeling effort. It uses a tailored objective function to calibrate the RDF parameters based only on the total stream flow measurements. In the following, we start by introducing the formulation of the objective function. Next, we test its validity, operationality, and robustness in adjusting the RDF parameters for long time series of stream flow (more than 30 years) on three gauging stations in the Meuse basin in Belgium. Then, we compare the results against those obtained by a standard adjustment method. Finally, we present a comparison of the baseflow hydrographs obtained using the new method with those produced by two more elaborate methods: CMB on two other gauging stations in the Meuse basin for which stream flow conductance measurements are available, and HGS on 64 synthetic catchments.

2 Materials and Methods

In this section, the governing equations of the RDF technique are first described (Sect. 2.1). Then, we explain the formulation of the new objective function used in the calibration of the filter parameters (Sect. 2.2). In Sect. 2.3, we briefly introduce the CMB technique used for evaluating our new approach. The other technique used to generate reference baseflows, i.e. the HGS model, is shortly presented in Sect. 2.4. Finally, we present the datasets used and the main characteristics of the watersheds draining at the studied gauging stations (Sect. 2.5).

2.1 Recursive Digital Filter equations

We used an improved formulation of Chapman (1991) filter, as proposed by Willems (2009). The original assumption of equal repartition of long-term volumes between baseflow and quick flow is generalized by parameterizing the flow fractions. The equations of the modified filter read:

$$\boldsymbol{f_{quick}(t)} = \frac{\left(1+\mathrm{e}^{-\frac{1}{k}}\right)w-\left(1-\mathrm{e}^{-\frac{1}{k}}\right)}{\left(1+\mathrm{e}^{-\frac{1}{k}}\right)w+\left(1-\mathrm{e}^{-\frac{1}{k}}\right)}\boldsymbol{f_{quick}(t-\Delta t)} + \frac{2w}{\left(1+\mathrm{e}^{-\frac{1}{k}}\right)w+(1-\mathrm{e}^{-\frac{1}{k}})}\left[\boldsymbol{q(t)}-\mathrm{e}^{-\frac{1}{k}}\boldsymbol{q(t-\Delta t)}\right] \quad (1a)$$

$$\boldsymbol{f_{base}(t)} = \mathrm{e}^{-\frac{1}{k}}\boldsymbol{f_{base}(t-\Delta t)} + \left(\frac{1-w}{2w}\right)(1-\mathrm{e}^{-\frac{1}{k}})\left[\boldsymbol{f_{quick}(t)}+\boldsymbol{f_{quick}(t-\Delta t)}\right] \quad (1b)$$

where $\boldsymbol{q(t)}$ [L^3 T^{-1}] is the measured stream flow time series, $\boldsymbol{f_{base}(t)}$ [L^3 T^{-1}] is the filtered baseflow time series, $\boldsymbol{f_{quick}(t)}$ [L^3 T^{-1}] is the filtered quick flow time series, k [T^{-1}] is the baseflow recession constant, and w [-] is the ratio of the quick

flow volume to the total stream flow volume. As can be seen in Eq. (1), parameter *w* should be at least greater than $\left(1-\mathrm{e}^{-\frac{1}{k}}\right)/\left(1+\mathrm{e}^{-\frac{1}{k}}\right)$.

The expression of $\boldsymbol{f_{base}(t)}$ can also be given as a function of $\boldsymbol{q(t)}$ by replacing $\boldsymbol{f_{quick}(t)}$ in Eq. (1b) by $\boldsymbol{q(t)-f_{base}(t)}$:

$$\boldsymbol{f_{base}(t)}=\frac{\left(1+\mathrm{e}^{-\frac{1}{k}}\right)w-\left(1-\mathrm{e}^{-\frac{1}{k}}\right)}{\left(1+\mathrm{e}^{-\frac{1}{k}}\right)w+\left(1-\mathrm{e}^{-\frac{1}{k}}\right)}\boldsymbol{f_{base}(t-\Delta t)}+\frac{(1-w)\left(1-\mathrm{e}^{-\frac{1}{k}}\right)}{\left(1+\mathrm{e}^{-\frac{1}{k}}\right)w+(1-\mathrm{e}^{-\frac{1}{k}})}\left[\boldsymbol{q(t)}+\boldsymbol{q(t-\Delta t)}\right] \quad (2)$$

In addition to the recession constant of baseflow, *k*, present in the original filter, another parameter *w* was introduced by Willems (2009) to represent the rainfall fraction contributing to quick runoff computed as an integral quantity over a long period as follows:

$$w=\frac{\sum_{t=t_0}^{t=t_N}\left[\boldsymbol{q(t)}-\boldsymbol{f_{base}(t)}\right]}{\sum_{t=t_0}^{t=t_N}\boldsymbol{q(t)}} \quad (3)$$

where t_0 [T] and t_N [T] are respectively the initial and final instants of the discharge series.

The two parameters to be determined to apply the RDF are the recession constant *k* and parameter *w*. The recession constant characterizes the shape of the baseflow graph, more specifically the rate of its depletion during periods of little to no precipitation. Parameter *w*, on the other hand, represents the remoteness of the baseflow from the total flow, which decreases with decreasing *w* values until both signals superimpose when *w* is set to zero.

2.2 Objective function for the RDF optimization

An original method is proposed to enable the determination of the RDF parameters in an automatic and reproducible way. Due to the lack of a direct reference, i.e. baseflow measurements, for the calibration of the filter parameters, we have encoded into a mathematical criterion the main elements involved in the visual inspection approach. We explain here the derivation of this criterion in four steps.

Step°1

Since the time series of stream flow and baseflow are supposed to superimpose during recession periods, the Nash-Sutcliffe Efficiency criterion E_{NSE} (Nash and Sutcliffe, 1970), calculated only on these periods, was used to evaluate the agreement between the two time series during recession periods:

$$E_{\mathrm{NSE}}=1-\frac{\sum_{i=1}^{i=N_r}\left(\sum_{t=t_{r0}^{i}}^{t=t_{rN}^{i}}\left(\boldsymbol{q(t)}-\boldsymbol{f_{base}(t)}\right)^2\right)}{\sum_{i=1}^{i=N_r}\left(\sum_{t=t_{r0}^{i}}^{t=t_{rN}^{i}}(\boldsymbol{q(t)}-\bar{q})^2\right)} \quad (4)$$

where $t_{r0}^{\,i}$ [T] and $t_{rN}^{\,i}$ [T] are respectively the initial and final instants of the i^{th} recession period, $\bar{q}$ [$L^3\,T^{-1}$] is the average flow rate on recession periods, and N_r [-] is the number of recession periods identified in the studied time series.

The recession periods were separated from other periods using an automatic algorithm similar to the one proposed by Vogel and Kroll (1996). It considers a recession to be a period over which the variation of a monthly smoothed flow signal does not exceed a certain threshold. This variation was calculated as the finite difference over each daily time step of this monthly averaged flow rate normalized by the watershed average flow rate divided by its surface area, with exponents 2 and 3/2 respectively:

$$\frac{\frac{\boldsymbol{q(t)-q(t-\Delta t)}}{\Delta t}}{\bar{Q}^2/_{A^{3/2}}} \leq s \tag{5}$$

with s [-] the threshold value of the non-dimensional temporal variation of total stream flow and $\bar{Q}$ [L^3 T^{-1}] is the mean flow rate. The influence of the value selected for s is detailed in Sect. 3.2.1.

Step°2

Since the RDF contains parameter w, which directly controls the distance between the total flow and the baseflow, using only criterion (4) for the calibration of the filter parameters would simply lead to a zero value for w. Indeed, this ensures a perfect fit between baseflow and total flow during recession periods (as expressed by Eq. (4)); but also outside recession periods, which is definitely not the sought result. Therefore, the optimization criterion must also reflect the fact that the baseflow differs from the total flow outside the recession periods. We expressed this through a composite Nash-Sutcliffe Efficiency criterion E'_{NSE}, which involves the ratio between the E_{NSE} criterion calculated on the recession periods ($E_{\mathrm{NSE}_{\text{recession periods}}}$) and a similar criterion calculated outside the recession periods ($E_{\mathrm{NSE}_{\text{other periods}}}$):

$$E'_{\mathrm{NSE}} = 1 - \frac{1 - E_{\mathrm{NSE}_{\text{recession periods}}}}{1 - E_{\mathrm{NSE}_{\text{other periods}}}} \tag{6}$$

Step°3

In Step 3, we describe three improvements brought to Eq. (6).

- First, to avoid a possible bias in the identification of the recession periods, we limited the calculation of criterion E_{NSE} on these periods to the final portion of the recession period, during which we may confidently presume that dominant baseflow conditions prevail. This was formalized by introducing parameter p [%] which represents the last portion of the duration of the recession period identified in Step 1. $E_{\mathrm{NSE}_{\text{other periods}}}$is thus calculated on all the remaining data, including the early parts of the recession periods (100-p)%.
- Second, an exponent β [-] was introduced to enable adjusting the relative weight given to criterion E_{NSE} calculated on the other periods compared to E_{NSE} calculated on the recession periods.
- Third, we applied criteria E_{NSE} on logarithmic transformed discharges to increase their sensitivity to low flow values.

The enhanced formulation $E_l{''}_{\mathrm{NSE}}$ of the composite criterion reads:

$$E_l{''}_{\mathrm{NSE}} = 1 - \frac{1 - E_{l_{\mathrm{NSE}_{\text{last } p\% \text{ of each recession period}}}}}{\left(1 - E_{l_{\mathrm{NSE}_{\text{other periods}}}}\right)^{\beta}} \tag{7}$$

The selection of the values of parameters p and β is discussed in Sect. 3.2.1.

Step°4

Criterion (7) does not contain any penalty if the calculated baseflow exceeds the measured total flow; instead of being lower than the total flow as expected. Therefore, we introduced another factor in the formulation of the objective function, in order to limit the exceedance of the total flow by the baseflow. This factor is calculated as the volume of baseflow exceeding the total flow normalized by the total stream flow volume. The formulation of this new criterion, *Exd*, was homogenized with that of criterion $E_l{''}_{\mathrm{NSE}}$ by subtracting the ratio of volumes from unity:

$$Exd = 1 - \frac{\sum_{i=1}^{i=N\mathrm{r}} \left(\sum_{t=t_{\mathrm{r_N}}^{i} - p(t_{\mathrm{r_N}}^{i} - t_{\mathrm{r_0}}^{i})}^{t=t_{\mathrm{r_N}}^{i}} (\boldsymbol{f_{\mathrm{base}}(t)} - \boldsymbol{q(t)})_{\boldsymbol{f_{\mathrm{base}}(t) > q(t)}} \right)}{\sum_{i=1}^{i=N\mathrm{r}} \left(\sum_{t=t_{\mathrm{r_N}}^{i} - p(t_{\mathrm{r_N}}^{i} - t_{\mathrm{r_0}}^{i})}^{t=t_{\mathrm{r_N}}^{i}} \boldsymbol{q(t)} \right)} \tag{8}$$

The final objective function G for calibrating the RDF parameters is thus defined as the product of the two proposed criteria:

$$G = E_l{''}_{\mathrm{NSE}} \times Exd \tag{9}$$

It should be noted that the two functions $E_l{''}_{\mathrm{NSE}}$ and *Exd* do not represent goodness-of-fit criteria in the traditional sense.

2.3 Improved CMB technique

Among the existing methods of baseflow separation, the conductance mass balance has been widely used for comparison (Lott and Stewart, 2016; Miller et al., 2015; Yu and Schwartz, 1999) or calibration (Lott and Stewart, 2016; Stewart et al., 2007; Zhang et al., 2013) of other techniques (e.g. graphical method) since it is considered more physically based and more objective. The CMB method relies on observed time series of stream flow rate and flow conductance. Subsurface flow is separated from surface flow using the dilution principle, the former being supposedly characterized by a high conductance and the latter by a low conductance:

$$\boldsymbol{f_{\mathrm{sub}}(t)} = \boldsymbol{q(t)} \frac{\boldsymbol{C_{\mathrm{q}}(t)} - C_{\mathrm{surf}}}{C_{\mathrm{sub}} - C_{\mathrm{surf}}} \tag{10}$$

where $\boldsymbol{f_{\mathrm{sub}}(t)}$ [L^3 T^{-1}] is the subsurface flow time series, $\boldsymbol{C_{\mathrm{q}}(t)}$ [T^3 I^2 L^{-3} M^{-1}] is the specific conductance time series of stream flow, C_{surf} and C_{sub} [T^3 I^2 L^{-3} M^{-1}] are the representative values of the specific conductance of surface flow and subsurface flow respectively. These conductance values are assumed to be stable signatures of the flow components and to differ significantly due to the distinct flow paths of each flow component.

Attention should be drawn to the difference between the flow components split by each of the RDF and the CMB method. The baseflow ($\boldsymbol{f}_{\mathbf{base}}$) separated by the RDF consists only of the flow in the saturated soil layer, whereas the subsurface flow ($\boldsymbol{f}_{\mathbf{sub}}$) separated by the CMB is the flow occurring in the saturated ($\boldsymbol{f}_{\mathbf{base}}$) and unsaturated ($\boldsymbol{f}_{\mathbf{inter}}$) soil layers. Thus, the quick flow component in the RDF ($\boldsymbol{f}_{\mathbf{quick}}$) consists of both the surface flow ($\boldsymbol{f}_{\mathbf{surf}}$) and the unsaturated flow ($\boldsymbol{f}_{\mathbf{inter}}$), while that of the CMB consists only of the surface flow ($\boldsymbol{f}_{\mathbf{surf}}$). So, any comparison between the two methods should be limited to periods where unsaturated flow contribution can be neglected.

The conductance parameters C_{surf} and C_{sub} are usually estimated from the observed stream flow conductance, at the moments of maximum and minimum flow respectively (neglecting the contribution of the other flow component to the total conductance at these moments). Before using CMB method as a reference for assessing our original calibration technique, we tested the validity of these two assumptions for determining the conductance parameters C_{surf} and C_{sub} (see Supplementary material). While assigning the maximum measured conductance to parameter C_{sub} was proved to be valid, the estimation of parameter C_{surf} directly from stream flow conductance at peak flow, assuming zero subsurface contribution, was found to bias the baseflow results. We fixed this issue using an original iterative method explained in the Supplementary material.

2.4 HGS model

HydroGeoSphere model was used by Li et al. (2014) to generate numerically the total flow and baseflow on 64 synthetic catchments. We compared these results with the baseflow filtered by our improved implementation of RDF. Since full details on the structure of the HGS model and its numerical implementation can be found in Therrien et al. (2010), only a short overview is provided here. HGS is a fully integrated Surface Water/Ground Water model that simulates the hydrological response of watersheds in a 3D physically based manner. Surface flow is simulated using the 2D diffusion approximation of the Shallow Water Equations (SWEs). Subsurface flow is simulated by the modified 3D Richard's equation. The interaction between the two flows is ensured through a conductance concept. All differential equations in the model are solved by means of a finite difference numerical scheme.

2.5 Data description

To assess the calibration procedure of the RDF based on the proposed objective function, we considered three gauging stations in river Ourthe, which is the main tributary of river Meuse in Belgium. The three stations correspond to nested watersheds sharing very similar land use properties (43% forests, 35% meadows, 5% agricultural areas, 2% urban areas and the remaining are water bodies). The other characteristics are presented in Table 1. These gauging stations were selected for the relatively long and uninterrupted available time series (hourly flow rates over 34 to 43 years).

We also used the CMB technique to assess its agreement with the new calibration method. Since this technique requires additional data on the stream flow conductance, which were not available for river Ourthe, we considered two watersheds in the catchment of river Hoyoux, another tributary of river Meuse in Belgium. As shown in Table 1, the specific conductance of the stream flow was monitored continuously between July 2013 and November 2015 at a time resolution of 15-min (Briers et al., 2016a, 2016b; Brouyère et al., 2016).

The raw data of flow rate and specific conductance were averaged to daily values to fit the needs of the baseflow separation processing carried out in this study.

Li et al. (2014) defined a synthetic V-catchment to assess the performance of different RDFs against baseflows modeled by the HGS model. Based on the plausible values considered for the physical catchment characteristics and the hydrological inputs, 70 distinct combinations of synthetic catchments were generated, some of which were then discarded for producing zero stream flow series. The numerical baseflows of these catchments will be compared in our study with the baseflow filtered by the improved implementation of the RDF. The characteristics of these catchments can be found in the Supplementary material of Li et al. (2014).

Table 1
Characteristics of the real watersheds

Catchment	Watershed	A [km^2]	I [%]	K_G [-]	Period of record	P_{10} – average – P_{90} of $\boldsymbol{q(t)}$ [m^3 s^{-1}]	min – average – max of $\boldsymbol{C_q(t)}$ [µS cm^{-1}]
Ourthe	Hotton	956.5	7.85	2.11	Jan 1979 – Dec 2012	1.95-15.43-36.20	N.A.
	Durbuy	1 220.3	7.38	2.43	Jan 1978 – Dec 2012	2.70-18.10-42.97	N.A.
	Tabreux	1 612.2	7.80	2.28	Jan 1970 – Dec 2012	3.36-22.27-52.85	N.A.
Hoyoux	Triffoy	30.3	4.50	2.09	Jul 2013 – Nov 2015	0.09-0.17-0.27	339 – 613 – 688
	Hoyoux upstream	94.3	4.50	1.98	Jul 2013 – Nov 2015	0.47-0.7-1.07	400 – 578 – 632

Note.
- P_{10} and P_{90} are respectively the 10th and 90th percentiles of the recorded daily rates of stream flow
- A is the watershed surface area
- I is the watershed average slope
- K_G is the Gravelius compactness coefficient is the ratio of the perimeter of the drainage basin to the circumference of a circle whose area is equal to that of the drainage basin that is used to characterize the basin shape (Bendjoudi and Hubert, 2002)

3 Results and discussion

In this section, we present and discuss the results of the calibration procedure of RDF using the proposed objective function (Eq. (9)). The ability of the procedure to identify the RDF parameters and estimate baseflow is first evaluated (Sect. 3.1).Next, we assess the sensitivity of the results to the value of parameters s, p and β used in the formulation of the objective function, as well as to the length of the considered time series (Sect. 3.2).

3.1 Assessment of the automatic calibration procedure of the RDF

Due to the unavailability of direct measurements of baseflow, standard approaches of validation do not apply to baseflow separation techniques. Therefore, as recommended in previous studies (e.g. Gonzales et al., 2009; Halford and Mayer, 2000; Lott and Stewart, 2016), we tested the proposed automatic calibration procedure in three ways:

1. Check the consistency and plausibility of the parameter values obtained for several gauging stations corresponding to nested watersheds;
2. Compare the computed parameter values with those derived from a standard graphical approach;
3. Compare the baseflow estimates with a reference baseflow computed by more elaborate methods:
   3.1. the tracer method CMB which incorporates supplementary real world observations (conductance measurements),

3.2. controlled numerical simulations using the physically based HGS model.

Comparisons 1 and 2 were undertaken for the three gauging stations in the Ourthe catchment, while comparison 3.1 could only be carried out for the Hoyoux stations for which flow conductance data are available, and comparison 3.2 was carried out on synthetic catchments for which total flows and baseflows were determined in Li et al. (2014) using the HGS model.

3.1.1 Ourthe catchment

The RDF calibration technique was tested for the three gauging stations Hotton, Durbuy, and Tabreux. A systematic exploration of the space of the filter parameters was undertaken to assess the variation of the objective function G for all possible combinations of k and w. Parameter k was assumed to range between 1 and 200 days, while parameter w may vary between 0.005 and 1. The parameters space was discretized using a 50 × 50 uniform grid. As shown in Fig. 1, the proposed objective function G varies substantially with the two parameters k and w, enabling thus an unambiguous detection of the optimum (marked by a red cross in Fig. 1). For the optimum found at each gauging station, Table 2 summarizes the values obtained for k, w, G as well as $E_l''_{\mathrm{NSE}}$ and Exd. The values taken by Exd reveal that the volume of computed baseflow exceeding the total stream flow corresponds to about 5% of the total volume, which is deemed relatively low.

Figure 1
Variation of the RDF objective function G as a function of k and w at the gauging stations of (a) Hotton, (b) Durbuy, and (c) Tabreux

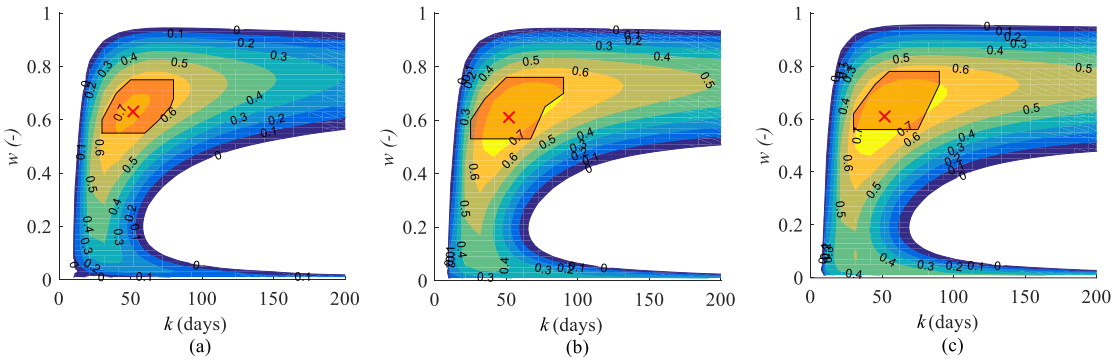

Relating the calibrated parameter values to the catchment characteristics is one way to gain primary confidence in the results. In the filter equations, parameter w reflects the partition of rainfall volumes in-between the different flow components. This partition is mainly influenced by watershed geomorphology and by the soil properties, which control the infiltration rate and the soil storage capacity. Since the three nested watersheds considered here share very similar characteristics in terms of average slope (Table 1) and land use (Sect. 2.4), the optimal value of parameter w is expected to remain similar at the three gauging stations. This is indeed the result that we obtained, as shown in Fig. 1 and Table 2: parameter w takes almost identical values in the three watersheds, corresponding to a quick flow volume of 61% to 63% of the total flow volume. For parameter k, the optimal values obtained for the three gauging stations are also almost identical, with a slight increase with the increasing watershed area (Table 2). Although this increase is hardly significant, it shows nonetheless a physically-consistent correlation between the recession timescale and the drainage area. Next, we checked whether the calibrated values of the RDF parameters are in agreement with the values derived from the widely used graphical method presented by Willems (2009), which is equivalent to the matching strip method. It consists

in (i) plotting the total flow on a logarithmic scale as a function of time, then (2) deducing the recession rate from the average of the inverse of all the slopes of the recession limbs. Parameter *w* is adjusted so that the magnitude of the estimated baseflow best approaches the total flow during recession periods. In Fig. 1, the sets of all (*k*,*w*) couples identified by this method are represented by a red shaded area. For the three studied gauging stations, the optimum obtained based on the objective function *G* (marker × in Fig. 1) falls within the range of possible combinations of *k* and *w* that a user would choose based on the graphical method. This result suggests that the proposed automatic approach remains consistent with the standard graphical one.

Table 2
Optimal values of the RDF parameters and the corresponding values of the objective function and its individual components

Watershed		Hotton	Durbuy	Tabreux
G	[-]	0.72	0.78	0.79
$E_l{''}_{\mathrm{NSE}}$	[-]	0.76	0.82	0.83
Exd	[%]	94.80	95.18	95.17
k	[days]	51	53	54
w	[-]	0.63	0.61	0.61

In addition, the proposed automatic method is perfectly reproducible, which is not the case of the standard graphical method, as it yields a relatively large range of acceptable values for each parameter (red shaded area in Fig. 1). It is therefore likely that, if the graphical analysis is repeated twice, even the same user would not pick exactly the same combinations of values for *k* and *w*. The difference in the level of determinism between the two methods is also examined in terms of baseflow estimates. In Fig. 2, we represent the envelope of the baseflow hydrographs filtered using the set of (*k*,*w*) parameters of the red shaded area in Fig. 1 obtained by the graphical adjustment and the baseflow filtered using the unique (*k*,*w*) couple of the proposed approach for Tabreux station between 2000 and 2010. This comparison illustrates the stochasticity of the baseflow estimation related to the absence of a well-defined criterion in the classical adjustment. To further evaluate our proposed approach in terms of baseflow estimates, we use hereafter the CMB technique, which enables a more physically based flow separation.

Figure 2
Comparison of baseflow time series obtained by RDF calibrated using the classical method and the method proposed in this paper on Tabreux station between 2000 and 2010

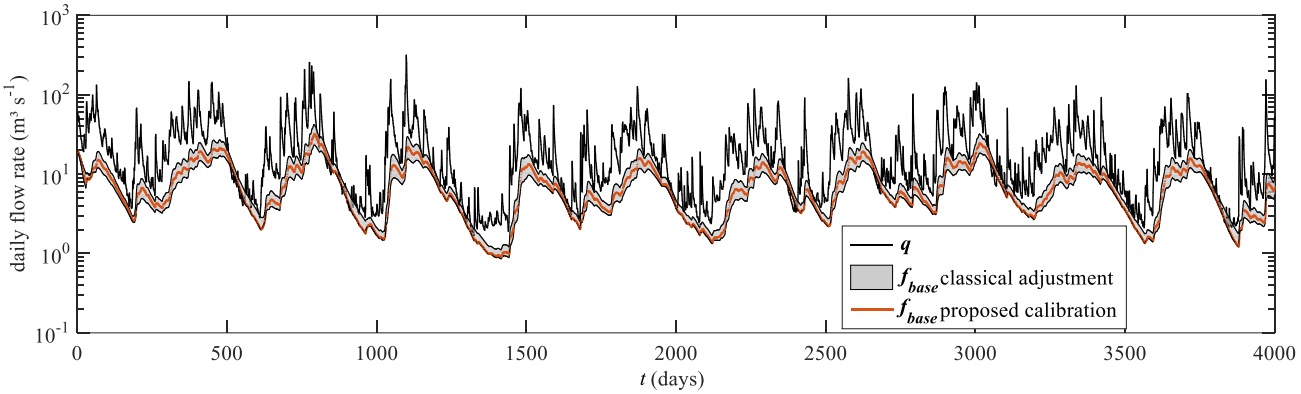

3.1.2 Hoyoux catchment

CMB method was applied at the gauging stations "Triffoy" and "Hoyoux upstream" to split the surface flow from the subsurface flow. For the two gauging stations, the following values of (C_{sub}, C_{surf}) were obtained: (650, 185) µS.cm^{-1} and (635, 57) µS.cm^{-1} respectively. Our new objective function Eq. (9) was also used, to calibrate the RDF and separate the baseflow from the quick flow at the two gauging stations. Since the outputs of the compared techniques do not represent exactly the same physical quantity, results were only compared in the lowest portion of each recession period, during which the baseflow is most probably the only contributor to stream flow.

To evaluate the agreement between the two techniques over these periods, we used the determination coefficient R^2 [-] calculated with respect to the RDF baseflow:

$$R^2 = 1 - \frac{\sum_{i=1}^{i=Nr}\left(\sum_{t=t_{rN}^{i}-p(t_{rN}^{i}-t_{r0}^{i})}^{t=t_{rN}^{i}}\left(\boldsymbol{f_{base/RDF}(t)} - \boldsymbol{f_{sub/CMB}(t)}\right)^2\right)}{\sum_{i=1}^{i=Nr}\left(\sum_{t=t_{rN}^{i}-p(t_{rN}^{i}-t_{r0}^{i})}^{t=t_{rN}^{i}}\left(\boldsymbol{f_{base/RDF}(t)} - \overline{\boldsymbol{f_{base/RDF}(t)}}\right)^2\right)} \quad (11)$$

In the last 50% of the identified recession periods, the results of the two methods are found generally close to each other, as they are both expected to represent the baseflow component only (Fig. 3). When computed relative to the RDF results, determination coefficients of 0.78 and 0.80 are obtained for "Hoyoux upstream" and "Triffoy" respectively. These values are considered relatively high given the difference of the concepts underlying the separation procedures: the RDF tends to extract a smoothly varying low frequency baseflow, whereas the CMB produces a noisier signal directly influenced by the dynamics of the total stream flow. In other words, the signal obtained by the CMB technique directly responds to all small fluctuations occurring during the recession periods, while that generated by the RDF does not due to its structural composition based on exponential averaging of total flow. The agreement between the two results is also shown by the scatter plots in Fig. 3, as most data fall within a ±10% interval around the agreement line.

Figure 3

Comparison of baseflow obtained by calibrated RDF and subsurface flow obtained by calibrated CMB method on (a) Triffoy for time series results, (b) Hoyoux upstream for time series results, (c) Triffoy for regression analysis, (d) Hoyoux upstream for regression analysis

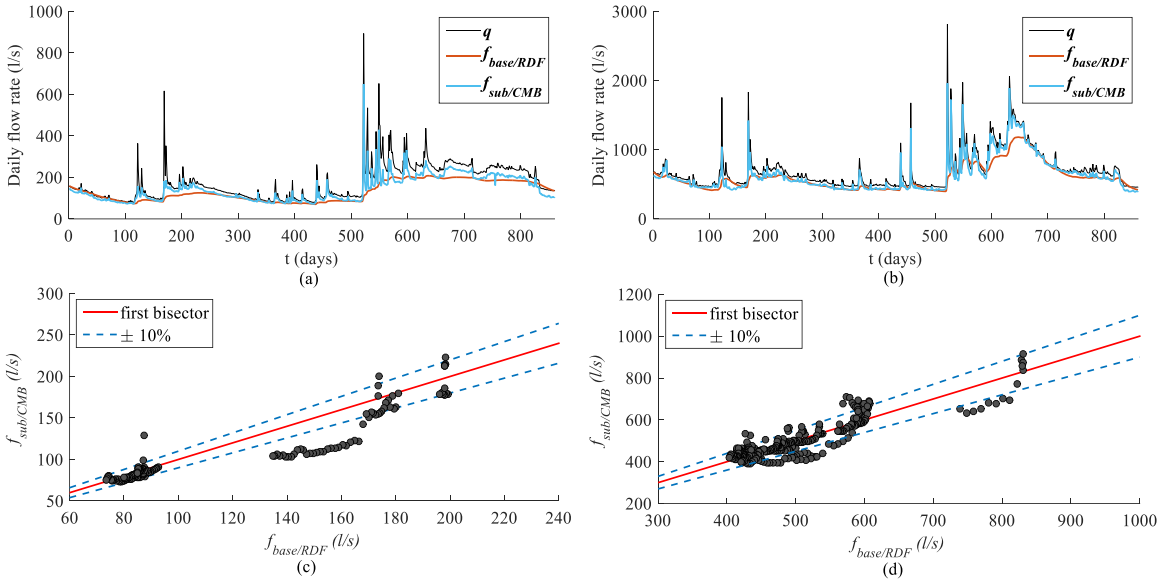

3.1.3 Synthetic catchments

For 64 synthetic catchments, we compare here the baseflow estimates obtained by our technique to baseflows generated numerically by Li et al. (2014) using the HGS model. As detailed in Fig. S3 in Supplementary material, the differences between the numerical estimates of baseflow and our filtered estimates was quantified using three criteria: (1) Nash-Sutcliffe criterion (E_{NSE}), (2) difference in the baseflow contribution to the total stream flow volume, and (3) correlation between the two baseflow estimates. For 28 catchments out of 64 (44%), we obtain a positive E_{NSE} value of which the overwhelming majority (86%) are above 0.6, implying a good agreement between filtered and numerical estimations. For 15 of the other catchments, a high overestimation of the baseflow integral contribution by the RDF relative to the numerical approach explains the relatively poor values obtained for E_{NSE}. Differences in the baseflow dynamics explain the lack of correspondence between the compared methods on 13 other catchments, while a different timing explains the poor agreement on the 8 remaining catchments.

A principal component analysis (PCA) was carried out on these groups as a function of the catchments characteristics (Fig. S4 and S5 in Supplementary material). It reveals a strong scatter of all groups in the principal component plane and hence no clear dependency of the results quality on the catchments characteristics. However, the weak performance of RDF could probably be explained by sporadic temporal variations of total flow on certain catchments that might affect the detectability of recession periods and thus the quality of baseflow estimates. Another recession detection method like the Automatic Baseflow Identification Technique (ABIT) developed by Cheng et al. (2016) could be tested in future research to check whether the highly fluctuating discharge flow could have biased the identification of recession periods and led to the poor agreement between filtered and numerical baseflows for some of the catchments.

3.2 Sensitivity analysis

In Sect. 3.2.1, we analyze the influence of parameters s, p and β on the calibrated values of the RDF parameters k and w, whereas the sensitivity of these values to the length of the available times series is discussed in Sect. 3.2.2.

3.2.1 Influence of the parameters involved in the calibration procedure

The first step for applying the proposed optimization procedure consists in identifying the recession periods in the studied time series, using the algorithm presented in Step 1 of Sect. 2.2. For this step, the non-dimensional slope threshold *s* was introduced to define the beginning and the end of recession periods. We discuss hereafter the influence of parameter *s* on the results of the automatic RDF calibration. We also tested the sensitivity of the calibrated parameters *k* and *w* to the values set for the selected percentage *p* of the recession period (taken from the end) and the relative weight β applied to the denominator of the $E_l{''}_{\mathrm{NSE}}$ criterion. We first substantiate the choice of the ranges of variation of parameters *s*, *p* and β to be considered for conducting the sensitivity analysis:

- A value slightly higher than zero is recommended for parameter *s* to reduce the algorithm sensitivity to small flow rate fluctuations which do not necessarily represent actual rainfall events. An interval of [1-10] for the slope threshold was found to be reasonable. The automatically identified recession periods were closely scrutinized to ensure that only falling limbs are captured, and only relatively long recessions are considered.
- Since the percentage parameter *p* is intended to ensure a pure baseflow condition, its value was upper limited to the second half of the identified recession periods, i.e. the last 50%. Furthermore, in order to have a sufficiently representative dataset of the receding shape of the flow rate during dry periods, a lower limit was set to 30%.
- Regarding the weighting exponent β, instead of supposing a default unity value, we checked whether small variations would significantly change the optimal values of the filter parameters *k* and *w*. Therefore, we studied the sensitivity of the results to its value in the range [0.7-1].

We scanned systematically the three dimensional space of parameters (*s*, *p*, and β), and we applied the proposed optimization method of RDF. The variation of the optimal values of (*k*,*w*) as a function of each parameter (*s*, *p*, and β) are displayed in Fig. S6 in the Supplementary material for the three gauging stations in the Ourthe catchment. For the considered ranges of variation of *s*, *p*, and β, these three parameters show a very low (Hotton station) to imperceptible (Durbuy and Tabreux stations) influence on the results of the optimization procedure.

- The negligible sensitivity of parameter *k* and *w* to the weight β (small error bars in Fig. S6 in the Supplementary material) shows that assigning different weights to different flow periods for the E_{NSE} criterion is needless and thus exponent β can be dropped from the objective function structure.
- Except for *w* at Hotton gauging station, parameter *p* has no influence on the optimal values of *k* and *w*. This suggests that the proposed identification of the recession periods is reliable.
- Similarly, the small influence of the slope threshold *s* on the optimal values of *k* and *w* highlights the adaptability and robustness of the proposed method to recession periods identification.

3.2.2 Influence of the time series length

Time series of 34 to 43 years are available at the three Ourthe gauging stations. These time series are relatively long compared to the records commonly available in other watersheds. Therefore, we analyzed the impact of using a shorter time series on the calibration procedure. To do so, we applied our automatic calibration method based on partial series of 2, 4, 6, 8, 10, 15 and 20 years. For each time series length, 14 to 41 continuous samples were randomly extracted

from the complete dataset and used to optimize parameters *k* and *w*. The variability in the computed optimal values of *k* and *w* for each time series length is shown in Fig. S7 in the Supplementary material. The boxplot representation displays the median of the results by means of a horizontal mark inside a box with edges corresponding to the 25th and 75th percentiles of the results. The whiskers extend up to the most extreme data points within 1.5 times the interquartile range away from the top and bottom of the box, and the outliers are plotted individually using the marker +.

Results show that adjusting the filter parameters on shorter datasets tend to overestimate the *k* value and slightly underestimate the *w* value with more dispersed estimations with smaller samples. For a 2-year dataset of continuous stream flow measurements, the optimal values of parameters *k* and *w* can be estimated with a maximum accuracy (between the 3 stations) of 12% and 22% respectively calculated as a Scaled Root Mean Square Error (E_{SRMSE} [-]):

$$E_{\mathrm{SRMSE}} = \frac{1}{X}\sqrt{\frac{1}{n}\sum_{i=1}^{n}(x_{\mathrm{i}} - X)^2} \tag{12}$$

where X is the parameter value calibrated on the whole dataset, x_{i} is the parameter value calibrated on the i^{th} reduced data sample (here two-year), and n is the number of reduced data samples (here 2-year) drawn from the entire population.

In order to better understand the variation of the optimization result as a function of the series length, the distribution obtained for each time series length is compared to the reference one obtained from the whole dataset. The comparison is made using a two sided Wilcoxon rank sum test at a statistical significance of 5%. All computed p-values were found to be well above 5%, indicating that the null hypothesis can be accepted for all compared couples and hence all samples can be considered drawn from the same distribution.

4 Conclusion

The main purpose of this study is to develop a practical and automatic method to implement one of the most commonly used techniques of baseflow separation, namely the RDF. We supposed that this objective can be best attained by a calibration procedure with an objective function expressing the phenomenological knowledge of the relation between the calibrated (baseflow) and the reference quantities (total flow) that has always been implicitly employed in the standard graphical procedures involving visual inspection. This function was devised using: (i) the time variation in the expected correspondence between the baseflow and the stream flow during dry and wet periods, and (ii) the upper limit imposed by the stream flow on the baseflow during recession periods. The finally adopted objective function is given in Eq. (9).

A series of validation tests were realized to assess the validity and robustness of the proposed method. The first verification was made on the optimizable property of the objective function, i.e. if it presents a clearly identifiable optimum in the parameters space. The second evaluation focused on the physical and numerical plausibility of the parameters values obtained at this optimum. The physical part was evaluated by comparing these values between several watersheds sharing the same geomorphological and soil characteristics, while the numerical part was evaluated by comparing these values with those obtained by a standard adjustment technique. The last validation procedure was

carried out on the baseflow hydrographs yielded by the proposed method. Due to the inaccessible nature of this flow component, results were compared to those extracted using more objective and elaborate methods, the CMB method and the HGS model. Another series of analysis was performed to test the robustness of the method to: (i) the identification of the recession periods needed in applying the new objective function, and (ii) the length of the discharge flow time series.

In its application on five watersheds of the Meuse basin in Belgium, the objective function showed a clear unique optimum with the associated parameters values being consistent with values obtained from more standard calibration methods and physically coherent between the studied watersheds. On the other hand, the good match between the baseflow estimates of RDF and CMB methods on two catchments and between RDF and HGS on 28 catchments suggests that the proposed formulation of the objective function is well adapted and reliable to calibrate the RDF parameters. The method was proved to be robust in terms of recession periods definition and length of flow time series. The main advantage of the developed calibration procedure is to combine a high degree of practicality and a low-cost (as for graphical methods) with a total reproducibility (as in tracer methods). In this respect, the developed method is not only more operational, but also more objective than standard graphical methods which involve visual inspection by the user.

Future research could focus on testing our new method on more catchments for which tracer-based hydrograph separation are available (Zhang et al., 2017), as well as investigating the applicability of the objective function developed here to separate different components of the quick flow i.e. overland flow from interflow. The relatively poor results of the comparison between RDF and HGS on some catchments should be further explored using another method of recession period identification (Cheng et al., 2016). Since all the analyses in this study were made on undisturbed watersheds with minor developments, it would be of high relevance to test the method validity and performance on more developed watersheds that are affected by human abstraction of groundwater or substantial land use changes.

Acknowledgements and Data

This work was partly funded by the ARC grant for Concerted Research Actions, financed by the Wallonia-Brussels Federation. It was also partly supported by the project MAR2WOLF awarded by the Research Council of the University of Liege. The Authors are grateful to the Department of Water and Environment of the Public Service of the Walloon Region (SPW) for providing data and funding the project on "Caractérisation complémentaire des masses d'eau dont le bon état dépend d'interactions entres eaux souterraines et de surface". The Authors deeply acknowledge the Editors and the anonymous Referees for their insightful comments and suggestions that helped us improve the quality of the manuscript.

The database of stream flow rates of the Ourthe watersheds are available in the online databank of the operational direction of the Walloon waterways (http://voies-hydrauliques.wallonie.be/opencms/opencms/fr/hydro/Archive/annuaires/index.html), and those of the Hoyoux watersheds are accessible from the website of the Walloon direction of non-navigable water courses (http://aqualim.environnement.wallonie.be/GeneralPages.do?method=displayStationsMap&time=2017-11-08%2011:50:34.873).

Competing interests

The authors declare that they have no conflict of interest.

References

Arnold, J. G., & Allen, P. M. (1999). Automated methods for estimating baseflow and ground water recharge from streamflow records. *Journal of the American Water Resources Association*, 35(2), 411–424. doi:10.1111/j.1752-1688.1999.tb03599.x

Barnes, B. S. (1939). The structure of base flow recession curves. *Earth and Space Science News*, 20(4), 721–725. doi:10.1029/TR020i004p00721

Bendjoudi, H. & Hubert, P. (2002). Le coefficient de compacité de Gravelius : analyse critique d'un indice de forme des bassins versants (Gravelius compactness coefficient: critical analysis of a shape index of watersheds). *Hydrological Sciences*, 47(6), 921–930. doi: 10.1080/02626660209493000

Beven, K. J. (1989). Changing ideas in hydrology: the case of physically-based models. *Journal of Hydrology*, 105(1–2), 157–172. doi:10.1016/0022-1694(89)90101-7

Briers, P., Orban, P., & Brouyère, S. (2016a). Quantification des échanges nappe-rivière pour les bassins tests (Quantification of groundwater-river exchanges in the tested basins). Délivrable D3.5 of the project "Caractérisation complémentaire des masses d'eau dont le bon état dépend d'interactions entre les eaux de surface et les eaux souterraines", Université de Liège. http://hdl.handle.net/2268/195405

Briers, P., Orban, P., & Brouyère, S. (2016b). Développement d'indicateurs des interactions entre eaux souterraines et eau de surface (Development of indicators for groundwater - surface water interactions) Délivrable D4.1 of the project "caractérisation complémentaire des masses d'eau dont le bon état dépend d'interactions entre les eaux de surface et les eaux souterraines". Université de Liège. http://hdl.handle.net/2268/195406

Brouyère, S., Briers, P., Schmit, F., Sohier, C., Degré, A., Descy, J.-P., Hallet, V., & Orban, P. (2016). Final report of the project "Caractérisation complémentaire des masses d'eau dont le bon état dépend d'interactions entre les eaux de surface et les eaux souterraines" (complemenary characterization of water bodies for which the good status depends on groundwater - surface water interactions). Université de Liège. http://hdl.handle.net/2268/195783

Brutsaert, W., & Nieber, J. L. (1977). Regionalized drought flow hydrographs from a mature glaciated plateau. *Water Resources Research*, 13(3), 637–643. doi:10.1029/WR013i003p00637

Cey, F. E., Rudolph, D. L., Parkin, G. W., & Aravena, R. (1998). Quantifying groundwater discharge to a small perennial stream in southern Ontario, Canada. *Journal of Hydrology*, 210(1–4), 21–37. doi:10.1016/S0022-1694(98)00172-3

Chapman, T. (1991). Comment on "Evaluation of automated techniques for base flow and recession analyses" by R. J. Nathan and T. A. McMahon. *Water Resources Research*, 27(7), 1783–1784. doi:10.1029/91WR01007

Cheng, L., Zhang L., Brutsaert W. (2016). Automated selection of pure base flows from regular daily streamflow data: Objective algorithm. *Journal of hydrological Engineering*, 21(11), 06016008. doi: 10.1061/(ASCE)HE.1943-5584.0001427

Daniel, J. F. (1976). Estimating groundwater evapotranspiration from streamflow records. *Water Resources Research*, 12(3), 360–364. doi:10.1029/WR012i003p00360

Eckhardt, K., Haverkamp, S., Fohrer, N., & Frede, H.-G. (2002). SWAT-G, a version of SWAT99.2 modified for application to low mountain range catchments. *Physical Chemistry of the Earth*, 27(9–10), 641–644. doi:10.1016/S1474-7065(02)00048-7

Ferket, B. V. A., Samain, S., & Pauwels, V. R. N. (2010). Internal validation of conceptual rainfall-runoff models using baseflow separation. *Journal of Hydrology*, 381(1–2), 158–173. doi: 10.1016/j.jhydrol.2009.11.038

Gonzales, A. L., Nonner, J., Heijkers, J., & Uhlenbrook, S. (2009). Comparison of different base flow separation methods in a lowland catchment. *Hydrology and Earth System Sciences*, 13(11), 2055–2068. doi:10.5194/hess-13-2055-2009

Halford, K. J., & Mayer, G. C. (2000). Problems associated with estimating ground water discharge and recharge from stream-discharge records. *Ground Water*, 38(3), 331–342. doi:10.1111/j.1745-6584.2000.tb00218.x

Hall, F. R. (1968). Base-Flow Recessions—A Review. *Water Resources Research*, 4(5), 973–983. doi:10.1029/WR004i005p00973

Holko, L., Herrmann, A., Uhlenbrook, S., Pfister, L., & Querner, E. P. (2002). Ground water runoff separation — test of applicability of a simple separation method under varying natural conditions. Paper presented at 4th International FRIEND Conference, International Association of Hydrological Sciences, Cape Town, South Africa.

Kunkle, G. R. (1968). A hydrogeologic study of the ground-water reservoirs contributing base runoff to Four Mile Creek east-central Iowa, U.S., Open File, Geological Survey Water-Supply, Rep. 1839-O, 41 pp.

Lang, C., Gille, E., Francois, D., & Drogue, G. (2008). Improvement of a lumped rainfall-runoff structure and calibration procedure for predicting daily low flow discharges. *Journal of Hydrology and Hydromechanics*, 56, 59–71.

Langbein, W. B. (1938). Some channel storage studies and their application to the determination of infiltration. *Earth and Space Science News*, 19(1), 435–445. doi:10.1029/TR019i001p00435

Li, Q., Xing, Z., Danielescu, S., Li, S., Jiang, Y., & Meng, F.-R. (2014). Data requirement of using combined conductivity mass balance and recursive digital filter method to estimate groundwater recharge in a small watershed, New Brunswick, Canada. *Journal of Hydrology*, 511, 658–664. doi:10.1016/j.jhydrol.2014.01.073

Lott, D. A., & Stewart, M. T. (2016). Base flow separation: A comparison of analytical and mass balance methods. *Journal of Hydrology*, 535, 525–533. doi:10.1016/j.jhydrol.2016.01.063

Matsubayashi, U., Velasquez, G. T., & Takagi, F. (1993). Hydrograph separation and flow analysis by specific electrical conductance of water. *Journal of Hydrology*, 152(1–4), 179–199. doi:10.1016/0022-1694(93)90145-Y

Miller, M. P., Johnson, H. M., Susong, D. D., & Wolock, D. M. (2015). A new approach for continuous estimation of baseflow using discrete water quality data: Method description and comparison with baseflow estimates from two existing approaches. *Journal of Hydrology*, 522, 203–210. doi:10.1016/j.jhydrol.2014.12.039

Nash, J. E., & Sutcliffe, J. V. (1970). River flow forecasting through conceptual models, Part I - A discussion of principles. *Journal of Hydrology*, 10(3), 282–290. doi:10.1016/0022-1694(70)90255-6

Nathan, R. J., & McMahon, T. A. (1990). Evaluation of automated techniques for base flow and recession analyses. *Water Resources Research*, 26(7), 1465–1473. doi:10.1029/WR026i007p01465

Nejadhashemi, A. P., Shirmohammadi, A., & Montas, H. J. (2003). Evaluation of streamflow partitioning methods, American Society of Agricultural and Biological Engineers, St. Joseph, Michigan, Las Vegas, Nevada, U.S., paper number 032183, ASAE Annual Meeting.

Peters, E., & Van Lanen, H. A. J. (2005). Separation of base flow from streamflow using groundwater levels illustrated for the Pang catchment (UK). *Hydrological Processes*, 19, 921–936, doi: 10.1002/hyp.5548

Pilgrim, D. H., Huff, D. D., & Steele, T. D. (1979). Use of specific conductance and contact time relations for separating flow components in storm runoff. *Water Resources Research*, 15(2), 329–339. doi:10.1029/WR015i002p00329

Pinder, G. F., & Jones, J. F. (1969). Determination of the ground-water component of peak discharge from the chemistry of total runoff. *Water Resources Research*, 5(2), 438–445. doi:10.1029/WR005i002p00438

Rorabaugh, M. I. (1964). Estimating changes in bank storage and ground-water contribution to streamflow. *International Association of Scientific Hydrology Publication*, 63, 432–441.

Rutledge, A. T., & Daniel, C. C. (1994). Testing an automated method to estimate ground-water recharge from streamflow records. *Ground Water*, 32(2), 180–189. doi:10.1111/j.1745-6584.1994.tb00632.x

Rutledge, A. T. (1997). Model-estimated ground-water recharge and hydrograph of ground-water discharge to a stream, U.S. Geological Survey, Reston, Virginia, U.S., Water Resources Investigations Report 97–4253, 29 pp.

Rutledge, A. T. (2005). The appropriate use of the Rorabaugh model to estimate ground-water recharge. *Ground Water*, 43(3), 292–293. doi:10.1111/j.1745-6584.2005.0022.x

Singh, K. P., & Stall, J. B. (1971). Derivation of base flow recession curves and parameters. *Water Resources Research*, 7(2), 292–303. doi:10.1029/WR007i002p00292

Stewart, M., Cimino, J., & Ross, M. (2007). Calibration of baseflow separation methods with streamflow conductivity. *Ground Water*, 45(1), 17–27. doi:10.1111/j.1745-6584.2006.00263.x

Su, C.-H., Costelloe, J. F., Peterson, T. J., & Western, A. W. (2016). On the structural limitations of recursive digital filters for base flow estimation. *Water Resources Research*, 52, 4745–4764. doi: 10.1002/2015WR018067

Tallaksen, L. M. (1995). A review of baseflow recession analysis. *Journal of Hydrology*, 165(1–4), 349–370. doi:10.1016/0022-1694(94)02540-R

Tardy, Y., Bustillo, V., & Boeglin, J. L. (2004). Geochemistry applied to the watershed survey: hydrograph separation, erosion and soil dynamics. A case study: the basin of the Niger River, Africa. *Applied Geochemistry*, 19(4), 469–518. doi:10.1016/j.apgeochem.2003.07.003

Tesoriero, A. J., Duff, J. H., Saad, D. A., Spahr, N. E., & Wolock, D. M. (2013). Vulnerability of streams to legacy nitrate sources. *Environmental Science and Technology*, 47(8), 3623–3629. doi:10.1021/es305026x

Therrien, R., McLaren, R. G., Sudicky, E. A., Panday, S. M. (2010). HydroGeoSphere : A three dimensional numerical model describing fully-integrated subsurface and surface flow and solute transport.

Toebes, C. & Strang, D. D. (1964). On recession curves, 1 - Recession equations. *Journal of Hydrology*, 3, 2–15.

Vogel, R. M., & Kroll, C. N. (1996). Estimation of baseflow recession constants. *Water Resources Management*, 10(4), 303–320. doi:10.1007/BF00508898

Wenninger, J., Uhlenbrook, S., Tilch, N., & Leibundgut, C. (2004). Experimental evidence of fast groundwater responses in a hillslope/floodplain area in the Black Forest Mountains, Germany. *Hydrological Processes*, 18(17), 3305–3322. doi:10.1002/hyp.5686

Willems, P. (2009). A time series tool to support the multi-criteria performance evaluation of rainfall–runoff models. *Environmental Modelling and Software*, 24(3), 311–321. doi:10.1016/j.envsoft.2008.09.005

Willems, P. (2014). Parsimonious rainfall–runoff model construction supported by time series processing and validation of hydrological extremes – Part 1: Step-wise model-structure identification and calibration approach. *Journal of Hydrology*, 510, 578–590. doi:10.1016/j.jhydrol.2014.01.017

Yu, Z. B., & Schwartz, F. W. (1999). Automated calibration applied to watershed-scale flow simulations. *Hydrological Processes*, 13(2), 191–209. doi:10.1002/(SICI)1099-1085(19990215)13:2%3C191::AID-HYP706%3E3.3.CO;2-E

Zhang, R., Li, Q., Chow, T. L., Li, S., & Danielescu, S. (2013). Baseflow separation in a small watershed in New Brunswick, Canada, using a recursive digital filter calibrated with the conductivity mass balance method. *Hydrological Processes*, 27(18), 2659–2665. doi:10.1002/hyp.9417

Zhang J. L.., Zhang Y. Q., Song J. X., & Cheng L. (2017). Evaluating relative merits of four baseflow separation methods in Eastern Australia. *Journal of Hydrology*, 549: 252–263. doi:10.1016/j.jhydrol.2017.04.004